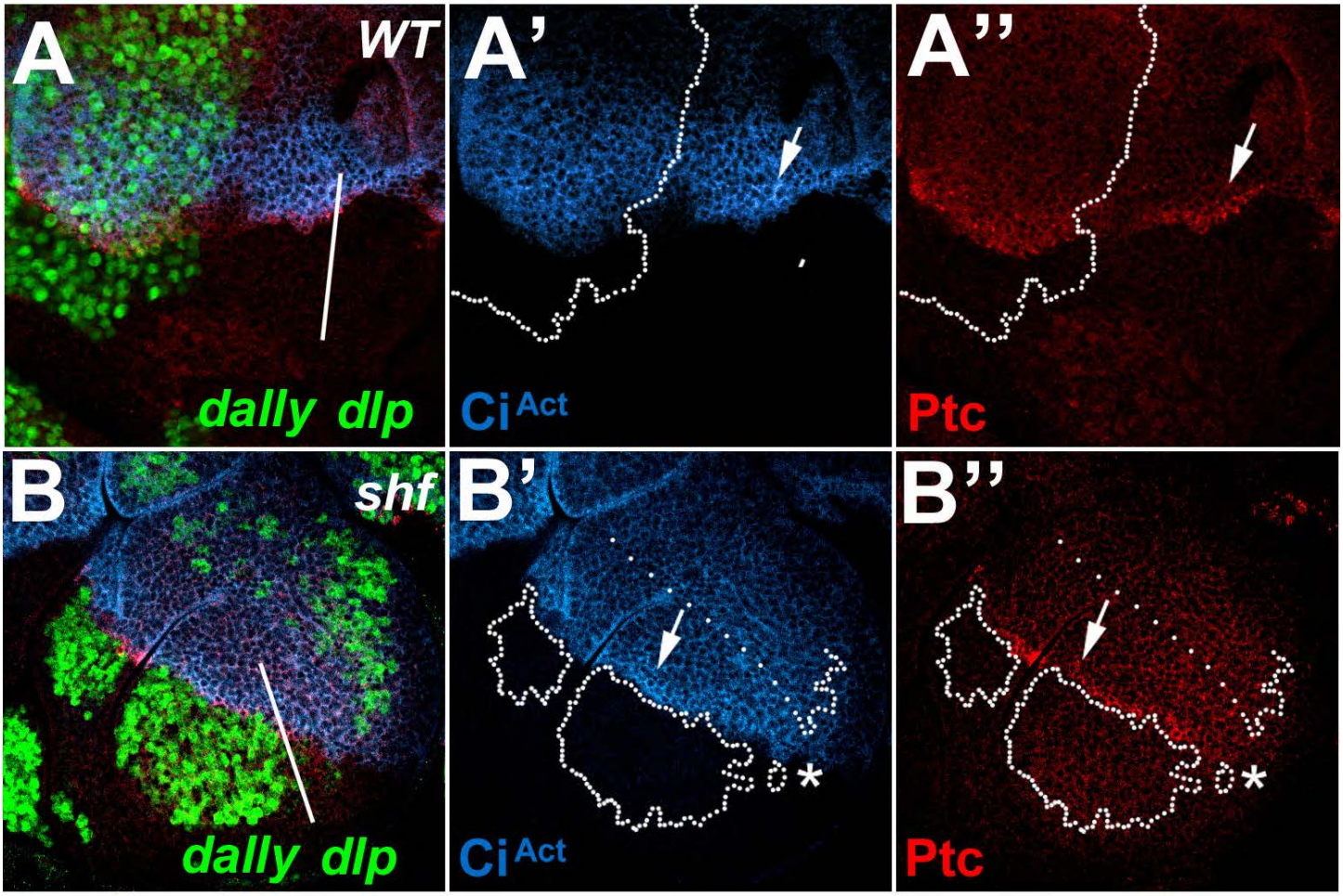

Fig. S1. Effects of losing *dally dlp* and *shf* on Hh signaling. *dally dlp* clones, marked by the absence of Myc epitope (green). Effects on Hh signaling are evaluated using Ci^{Act} (blue) and Ptc (red). (**A-A″**) In wild-type disc, double-sided clones lacking both glypicans strongly reduce long-range, but not short-range, signaling. (**B-B″**) In *shf* mutant discs, high levels of Ci^{Act} and Ptc are lost from double-sided *dally dlp* mutant clones (asterisks), but the thin Ci^{Act} and Ptc stripes typical of *shf* discs are retained in anterior clones that are touching wild-type, *dally dlp* containing posterior cells (arrows in B′,B″).

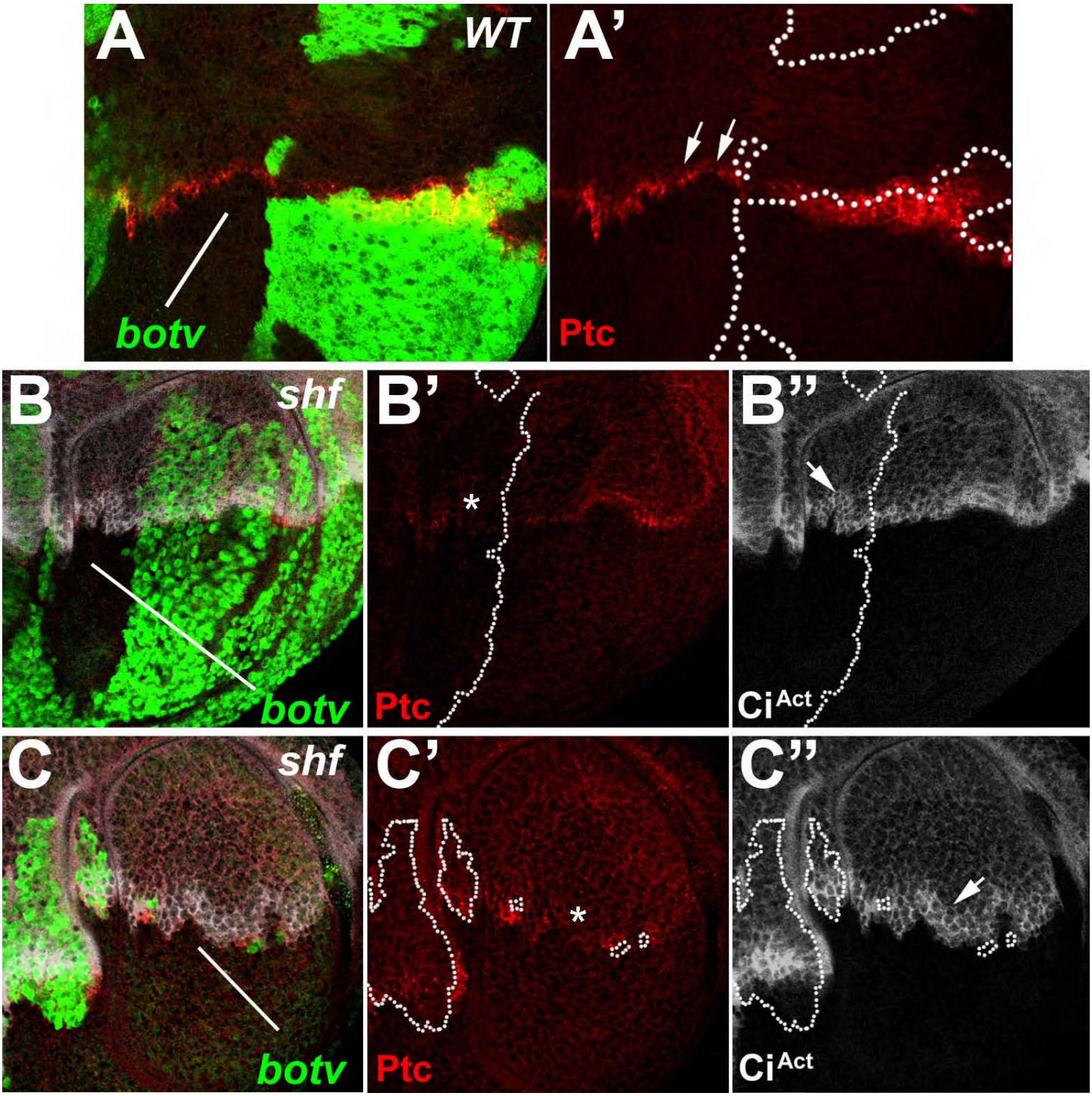

Fig. S2. Hh signaling defects in wild-type and *shf* cells lacking HS synthesis. (**A,A′**) *botv* clones, identified by the absence of GFP (green), in wild-type disc. In the region with double-sided clones, Ptc is reduced to a thin stripe. (**B-C″**) *shf* discs with *botv* clones, identified by the absence of GFP (green). Ptc (red) is lost from regions with double-sided clones, but in the same area the width of the Ci^{Act} stripe (white) is not reduced (arrows).

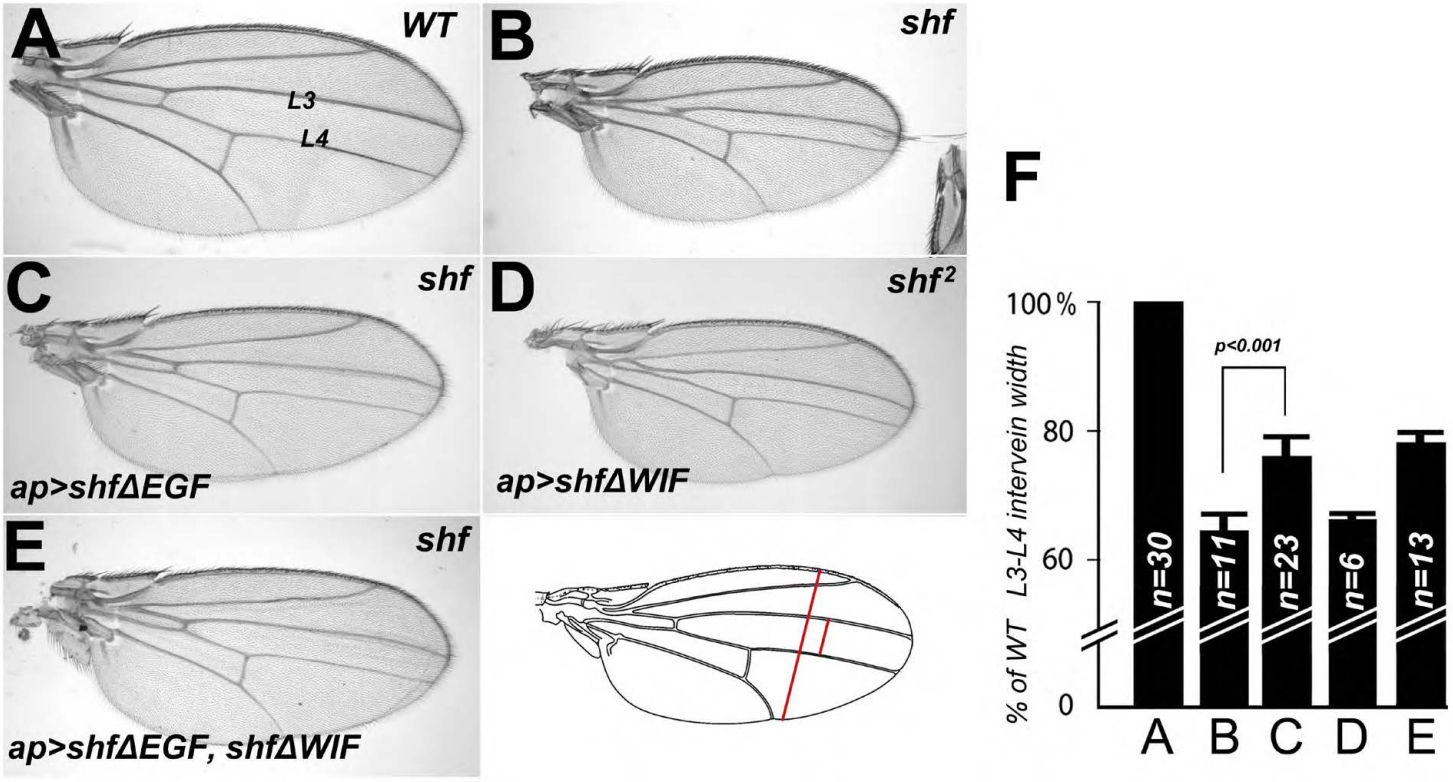

Fig. S3. Effects of expressing the 'WIF' and 'EGF-like' domains of Shf on of the Hh-dependent L3-L4 spacing in *shf* wings. (**A**) Wild-type wing showing normal spacing between L3 and L4 veins. (**B**) In *shf* mutant wings, L3 and L4 are much closer together. (**C-E**) Changes in L3-L4 spacing after *ap-Gal4*-driven expression of truncated Shf constructs in *shf* mutants. Because null shf^{x33}/Y flies expressing *UAS-shfΔWIF* did not survive to adulthood, we expressed it in shf^{2}. (**F**) Quantification of changes in L3-L4 spacing in the genotypes of A-E. L3-L4 distances were normalized to the anterior-posterior width of the entire wing (red lines in wing diagram), then expressed as percentages of the normalized wild-type L3-L4 distance. L3-L4 spacing in *shf* wings was improved only in the presence of ShfΔEGF, whereas expression of *UAS-shfΔWIF* did not improve spacing in comparison with either shf^{2} or shf^{x33}. Differences of statistical significance were determined using the Mann-Whitney U-test. Similar results were obtained with *en-Gal4* (Avanesov et al., 2012).

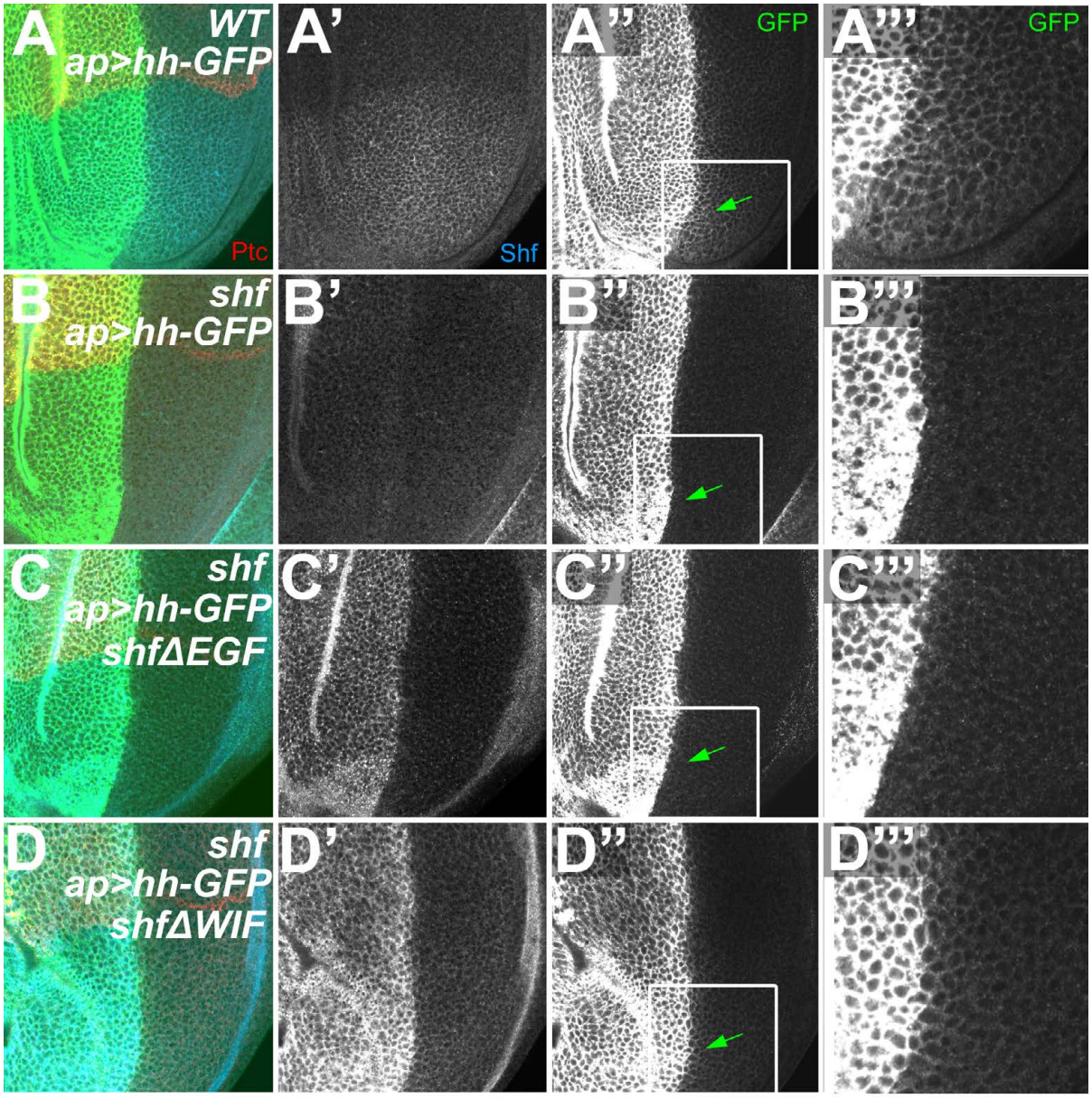

E **Normalized Hh-GFP accumulation in ventral-posterior quadrant (VP/VA)**

wt, ap>hh-GFP	1.6 +/- 0.3 (N=15)		
shf, ap>hh-GFP	1.2 +/- 0.1 (N=11)	P=0.18	
shf, ap>hh-GFP, shfΔEGF	1.2 +/- 0.2 (N=12)		P= 0.004
shf, ap>hh-GFP, shfΔWIF	1.4 +/- 0.2 (N=10)		P= 0.045

Fig. S4. Effects of truncated Shf constructs on Hh-GFP movement. (**A-D**) Wing pouch and detail images of wing discs from Fig. 3G-J, with dorsal *ap-Gal4*-driven expression of *UAS-hh-GFP*. Panels show Hh-GFP (green or white), Shf (blue or white) and Ptc (red). Hh-GFP in found well into the ventral compartment in wild type (A-A‴), but is largely absent ventrally in *shf* (B-B‴). *UAS-shf*Δ*EGF* does not significantly increase ventral Hh-GFP in *shf* disc (C-C‴), but *UAS-shf*Δ*WIF* does (D-D‴). (**E**) Average intensity values of Hh-GFP in ventral-posterior (VP) quadrant, normalized to the values in the ventral-anterior quadrant (VA) distant from the dorsal zone of Hh-GFP expression. Hh-GFP does not move as far in the anterior, probably due to binding to anteriorly expressed Ptc. Shown are standard deviations, numbers of images scored and significance of selected comparisons using the two-tailed Student's *t*-test.

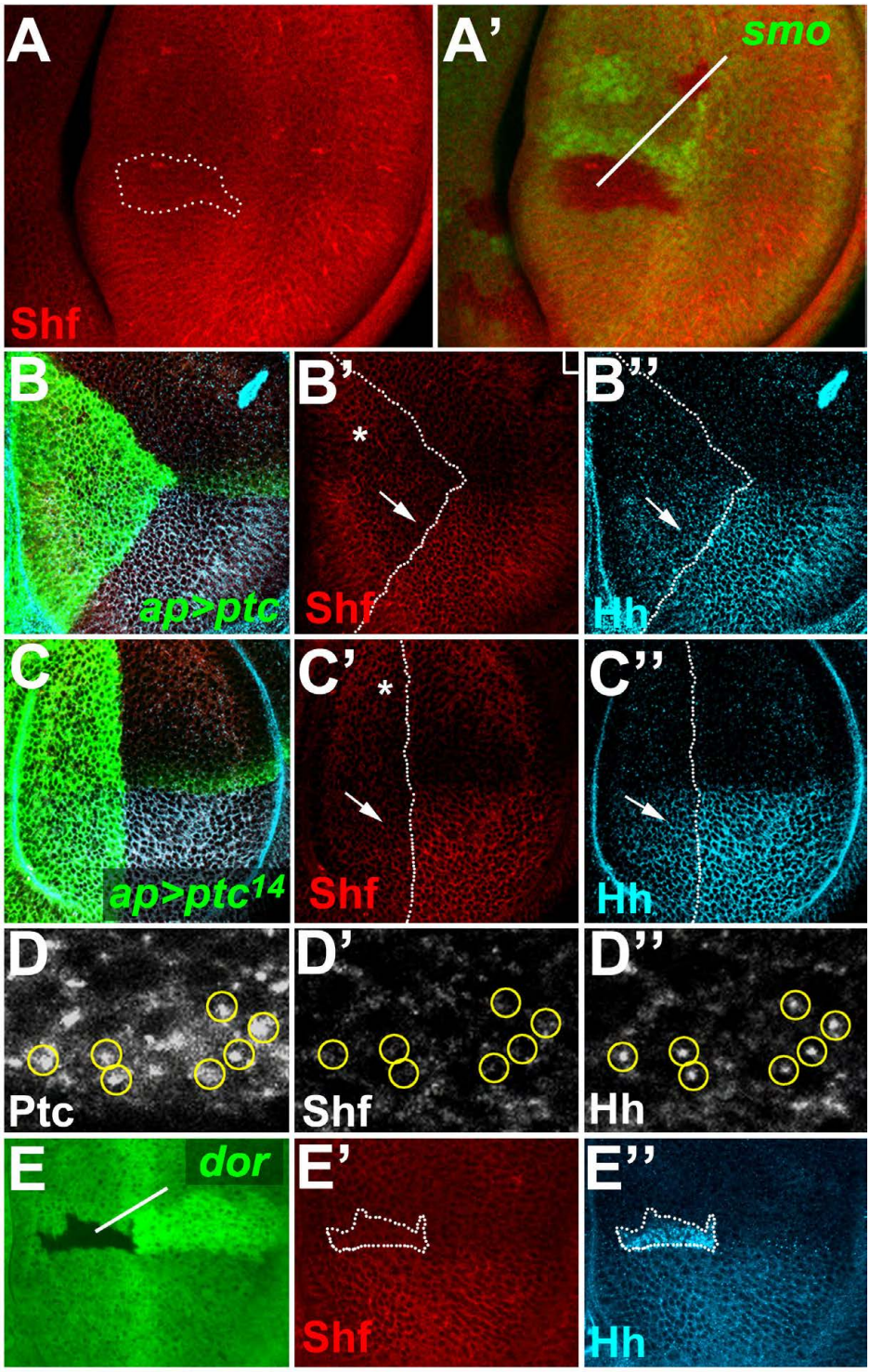

Fig. S5. Effects of Hh receptors and Hh signal transduction on Shf accumulation. (**A**,**A**′) Anti-Shf staining (red) does not change in *smoothened* (*smo*) mutant clone (identified by the absence of GFP, green) of anterior origin along the anterior-posterior compartment boundary, despite the loss of all Hh signaling within the clone. (**B-B**″) Dorsal *ap-Gal4*-driven overexpression of *UAS-ptc.* Discs were stained for Ptc (green), Shf (red) and Hh (blue). Owing to dominant-negative effects of the wild-type receptor on Hh signaling and Hh targets, this decreases growth of the dorsal compartment. Anti-Shf staining (red) is not increased by the excess Ptc, and in the posterior is reduced (arrows), along with anti-Hh staining (blue). Shf levels are not changed by *UAS-ptc* in the far anterior compartment (asterisk in B′), where Hh levels are low. (**C-C**″) Dorsal *ap-Gal4*-driven expression of the internalization defective Ptc^{14} allele (marked with anti-Ptc, green). This reduces anti-Shf (red) and anti-Hh (blue) staining in the posterior compartment (arrows in C′ and C″). Anti-Shf staining is not changed by Ptc^{14} expression in the far anterior compartment (asterisk in C′). (**D-D**″) Anterior cells at the anterior-posterior boundary of a wild-type disc show distinct Ptc- and Hh-positive puncta that do not include Shf. (**E-E**″) dor^{8} mutant clones, identified by the absence of green GFP, increase anti-Hh staining (blue) and anti-Ptc staining (not shown), but do not affect anti-Shf staining (red).

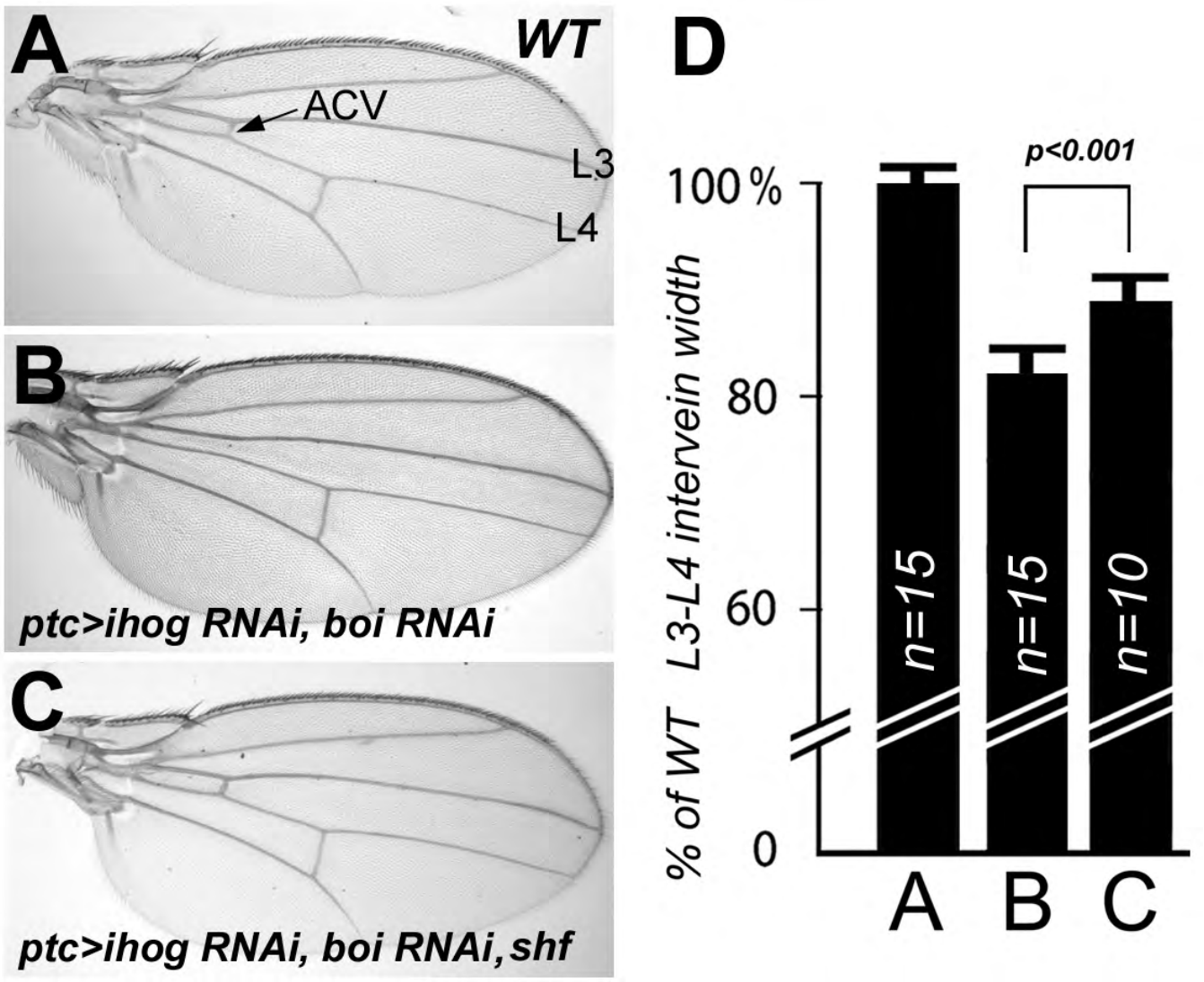

Fig. S6. Influence of *shf* overexpression on the effects of *ihog/boi* knockdown on L3-L4 spacing. (**A-C**) Adult wings from wild type (A), and after anterior *ptc-Gal4*-driven knockdown of *ihog* and *boi* levels using *UAS-ihog-RNAi* and *UAS-boi-RNAi*. *ihog* and *boi* knockdown reduces L3-L4 spacing (B), but this is partially rescued by overexpression of *UAS-shf* (C). (**D**) Quantification of changes in L3-L4 spacing in the genotypes of A-C. L3-L4 distances were normalized as in Fig. S3. Error bars show s.d. The improvement in L3-L4 in C compared with B was highly significant using Student's *t*-test. *ptc-Gal4* wings expressing *UAS-shf* alone had average L3-L4 distances that were slightly lower than wild type, although not significantly so (not shown, P=0.28).

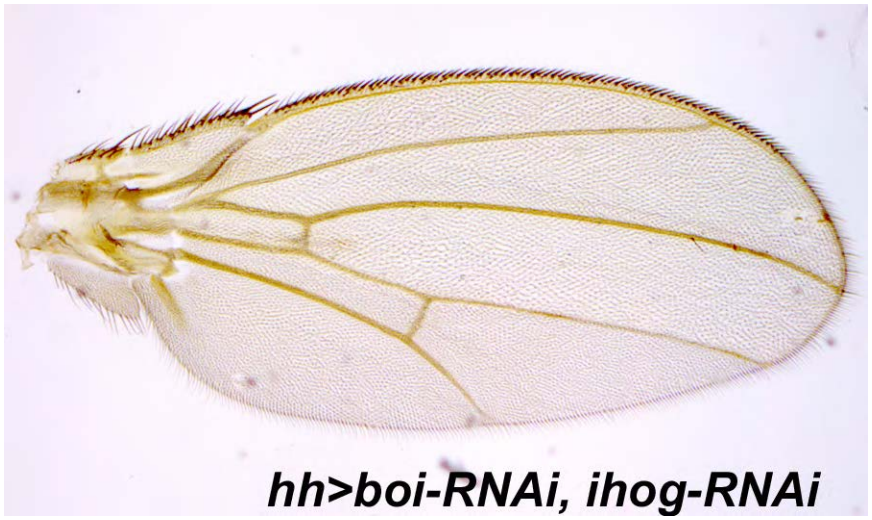

Fig. S7. Adult wing after posterior knockdown of *ihog* and *boi* expression. Posterior-specific knockdown of *ihog* and *boi* expression using *hh-Gal4*-driven expression of *UAS-ihog-RNAi* and *UAS-boi-RNAi* does not reduce the distance between the third and fourth longitudinal veins, an indicator of Hh signaling, despite the reduced size of the posterior compartment.